EFDA–JET–PR(13)35

I.T. Chapman, D. Brunetti, P. Buratti, W.A. Cooper, J.P. Graves, J.R. Harrison,
J. Holgate, S. Jardin, S.A. Sabbagh, K. Tritz, the MAST and NSTX Teams
and JET EFDA contributors

Three Dimensional Distortions of the Tokamak Plasma Boundary: I. Boundary Displacements in the Presence of Saturated MHD Instabilities

Three Dimensional Distortions of the Tokamak Plasma Boundary: I. Boundary Displacements in the Presence of Saturated MHD Instabilities

I.T. Chapman[1], D. Brunetti[2], P. Buratti[3], W.A. Cooper[2], J.P. Graves[2], J.R. Harrison[1], J. Holgate[1,4], S. Jardin[5], S.A. Sabbagh[6], K. Tritz[7], the MAST and NSTX Teams and JET EFDA contributors*

JET-EFDA, Culham Science Centre, OX14 3DB, Abingdon, UK

[1]*EURATOM-CCFE Fusion Association, Culham Science Centre, OX14 3DB, Abingdon, OXON, UK*
[2]*CRPP, Association EURATOM/Conf´ed´eration Suisse, EPFL,1015 Lausanne, Switzerland*
[3]*Associazione EURATOM-ENEA sulla Fusione, CR Frascati, Roma, Italy*
[4]*AUniversity of Cambridge, Department of Physics, Cavendish Laboratory, J.J. Thomson Avenue, Cambridge, CB3 0HE, UK*
[5]*PPPL, Princeton University, PO Box 451, Princeton, NJ 08543, USA*
[6]*Department of Applied Physics and Applied Mathematics, Columbia University, New York, USA*
[7]*John Hopkins University, Baltimore, MD, USA*
** See annex of F. Romanelli et al, "Overview of JET Results", (24th IAEA Fusion Energy Conference, San Diego, USA (2012)).*

Preprint of Paper to be submitted for publication in Nuclear Fusion

Abstract.

The three dimensional plasma boundary displacement induced by long-lasting core MHD instabilities has been measured in JET, MAST and NSTX. Only saturated instabilities are considered here since transient rapidly-growing modes which degrade confinement and act as potential triggers for disruptions bring more fundamental concerns than boundary displacements. The measured displacements are usually small, although in extreme cases in MAST when the rotation braking is strong and a significant global displacement can be observed. The instability most likely to saturate and exist for many energy confinement times whilst distorting the boundary of ITER is the saturated internal kink, or helical core, which can be found in plasmas with a wide region of low magnetic shear such as the hybrid scenario. This mode can lead to non-negligible boundary displacements. Nonetheless, the boundary displacement resultant from core MHD instabilities in ITER is predicted to be less than $\pm 1.5\%$ of the minor radius, well within tolerable limits for heat loads to plasma facing components, though greater than the perturbation allowable for high coupled ICRH power.

1. Introduction and Background

There are various conditions under which fusion plasmas are susceptible to long-lasting plasma instabilities which can give rise to displacements of the plasma boundary. For the purposes of this study, we discount any displacements arising due to transient events since these distortions are especially hard to model numerically and therefore extrapolation of probable distortions in ITER is problematic. It has been observed in many devices that in plasmas with a wide region of low magnetic shear and $q \geq 1$, the plasma exhibits long-lasting $n = 1$ ideal MHD instabilities [1, 2, 3, 4, 5, 6, 7]. Similarly, neoclassical tearing modes can exist for multiple energy confinement times [2, 9, 10, 11] and resistive wall modes controlled by magnetic feedback can also be sustained for a long time [12, 13, 14, 15]. Routinely, the boundary displacement due to such instabilities is of secondary concern, even though it does lead to a noticeable level of non-axisymmetry and can cause large displacements under certain conditions.

However, such perturbations to the boundary could lead to unacceptable heat loads on the plasma facing components in ITER. The allowable plasma displacement to avoid damage to the first wall has been assessed as 8cm with three-dimensional scrape-off layer transport modelling [16], whilst the boundary must stay within a 4cm envelope of its set-point to achieve good RF coupling [17]. Consequently it is important that we can predict the likely distortions in ITER and prepare methods for the avoidance or control of such boundary displacements.

Measurements of the displacements caused by core MHD are described in section 2 and compared to numerical modelling in section 3. Then predictions for the displacements expected in ITER due to core MHD are made in section 4 before the implications of the work are discussed in section 5.

2. Measurements of displacements due to core MHD in present machines

2.1. Internal $n/m = 1/1$ kink modes

In this section we are only concerned by edge displacements due to saturated core MHD instabilities. Edge displacements have been measured with the multi-energy soft X-ray (ME-SXR) system on NSTX in the presence of core-localised $n = 1$ internal kink and tearing modes. The multi-energy soft X-ray cameras have 1cm radial resolution between channels near the plasma edge, and interpolation allows sub-cm resolution. An $n = m = 1$ internal kink mode in plasmas with low-shear above $q = 1$ has been found to couple to $m/n = 2/1$ tearing modes, giving rise to islands of 10cm, equating to 15% of the minor radius [18]. The position of the boundary in the presence of a 1/1 kink coupled to a 2/1 tearing mode as measured by the ME-SXR system, which can persist for half the length of the plasma discharge in NSTX, is illustrated in figure 1. It is evident that the plasma boundary is distorted by $\pm$7.5mm, or $\pm$1.3% of the minor radius.

MAST plasmas with a safety factor above unity and a profile with either weakly

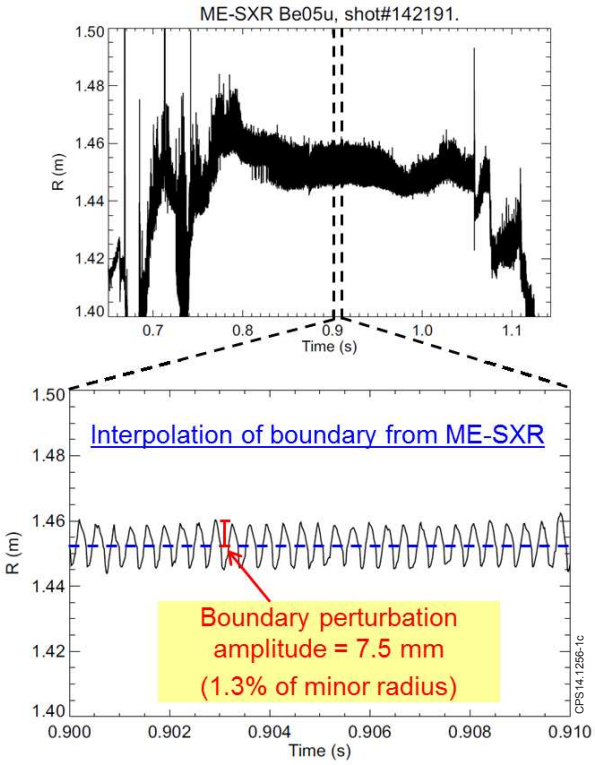

Figure 1. The plasma boundary measured by the Multi-Energy Soft X-ray system in NSTX for a discharge with a core saturated 1/1 kink mode coupled to a 2/1 tearing mode, showing a displacement of 1.3% of the minor radius.

reversed shear, or broad low shear regions, regularly exhibit long-lived saturated ideal magnetohydrodynamic (MHD) instabilities [1]. The toroidal rotation is flattened in the presence of such perturbations and the fast ion losses are enhanced [19]. These ideal long-lived modes (LLMs), distinguished as such by the notable lack of islands or signs of reconnection, are driven unstable as the safety factor approaches unity. This could be of significance for advanced scenarios, or hybrid scenarios which aim to keep the safety factor just above rational surfaces associated with deleterious resistive MHD instabilities, especially in spherical tokamaks which are susceptible to such ideal internal modes for q_{min} further above a rational surface than conventional aspect ratio devices.

Under typical circumstances the long-lived kink mode (LLM) seen in MAST plasmas with broad low-shear q-profiles [1] does not significantly perturb the plasma boundary. However, there are circumstances under which significant edge perturbations are observed. For instance, figure 2 shows the D_α light measured by the fast visible camera as a function of tangency radius at the midplane in MAST in the presence of an $n = 1$ kink mode. As the mode rotates past the field of view of the camera, the plasma boundary moves in and out by 3-4cm, equating to 4-6.5% of the minor radius. Here, the exposure time of the camera was 2μs whilst the temporal resolution was 500Hz. The spatial resolution is approximately 3mm. The CCD camera directly images visible light photons using a wide field of view lense. The camera location was determined by

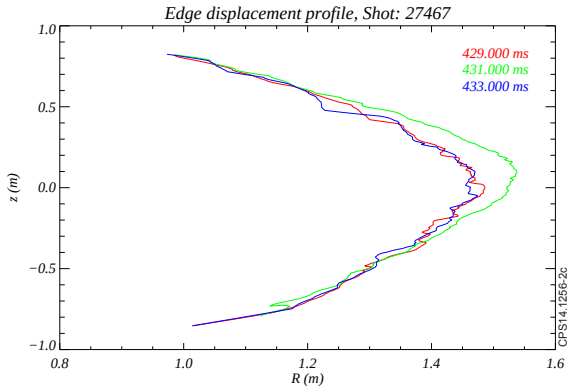

Figure 2. MAST The plasma boundary measured by high-speed visible imaging in MAST showing the distortions in the presence of saturated core MHD activity.

reference to the location of known features inside the vessel in the image plane and within a 3D co-ordinate system with MAST at its centre. The camera location and field of view then allow the radius at which camera lines of sight are tangent to flux surfaces to be calculated, giving the local plasma brightness as a function of radius. The boundary is found using the part of the camera image from the X-point going outboard, and finding the maximum brightness for each row of pixels in the camera image, and recording the (R, Z) location of where the brightest pixel is tangent to circular flux surfaces. When the plasma is rotating quickly, the distortion is confined to the plasma core, whereas at low rotation, the plasma boundary can become significantly perturbed. Often, such large distortions lead to plasma terminations, though there are rare occasions when the plasma survives and the safety factor evolution results in the decay of the mode.

Figure 3 shows how the core plasma rotation profile is degraded by the presence of a long-lived mode. Such strong rotation braking was attributed to the neoclassical viscous torque arising from the non-axisymmetry introduced by the $n = 1$ core distortion [19, 20]. The saturated amplitude of the mode was estimated by comparing experimental SXR data to simulations for different eigenstructure amplitudes, enabling the calculation of the braking torque according to the NTV theory [21]. The result is in good accordance with the measured braking, except at rational surfaces [19, 20]. Here, the mode's eigenstructure is expected to be intransigent as it saturates [22, 23], and the effect of enhanced fast ion losses is neglected.

The boundary displacement is found to correlate strongly with the plasma rotation. Whilst the boundary displacement in the presence of the LLM is usually sub-cm, it can become as large as 4cm at very low plasma rotation, though in a large majority of cases this does result in plasma disruption. Figure 4 shows the boundary displacement measured in MAST as a function of the plasma rotation at the radial position of the minimum in safety factor for non-disruptive cases. Here the boundary displacement is measured using visible imaging. For a few points, the measurement is taken as the average of the visible imaging and that from the Thomson scattering, which provides

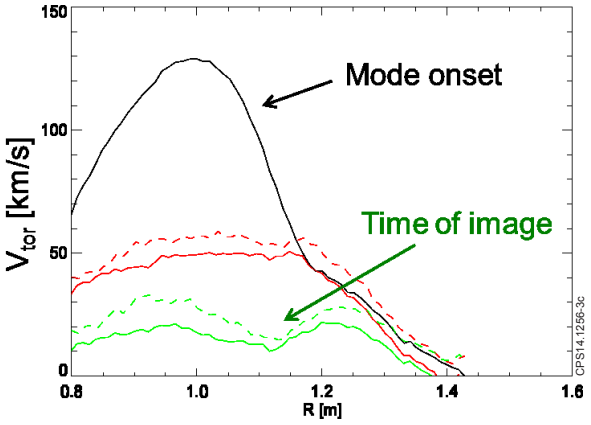

Figure 3. The plasma toroidal velocity profile measured by Charge Exchange Recombination Spectroscopy in MAST. The time slice corresponding to the boundary shape shown in figure 2 is marked in green.

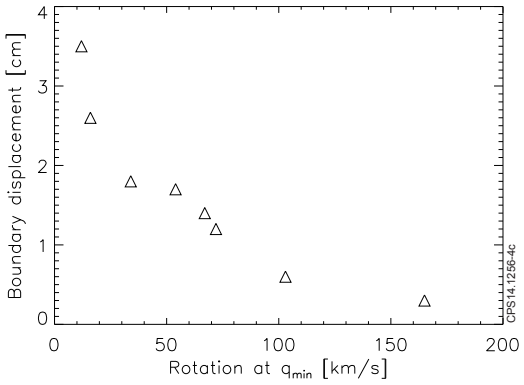

Figure 4. The edge displacement in MAST as a function of the toroidal velocity at the radial position of the minimum in safety factor.

complementary data only when the diagnostic lasers were used in burst mode and separated by only a few μs, making it possible to resolve the distortion associated with the high-frequency LLM oscillation. Whilst it was shown that the rotation does not strongly influence the linear growth rate of the $n = 1$ kink mode in reference [1], these simulations do not account for the effect of the nonlinear saturated state nor the interaction between the NTV braking and the mode evolution. It is evident that the boundary displacement associated with the LLM increases as the plasma rotation decreases, meaning that for accurate prediction in ITER, nonlinear modelling which includes the braking associated with the non-axisymmetry introduced by core MHD is needed.

Since ITER is likely to rotate at much slower velocities than present-day machines, one could infer from figure 4 that the edge displacement due to saturated $n = m = 1$ kink modes, as likely with broad low-shear q-profiles [24], may be large. However, it

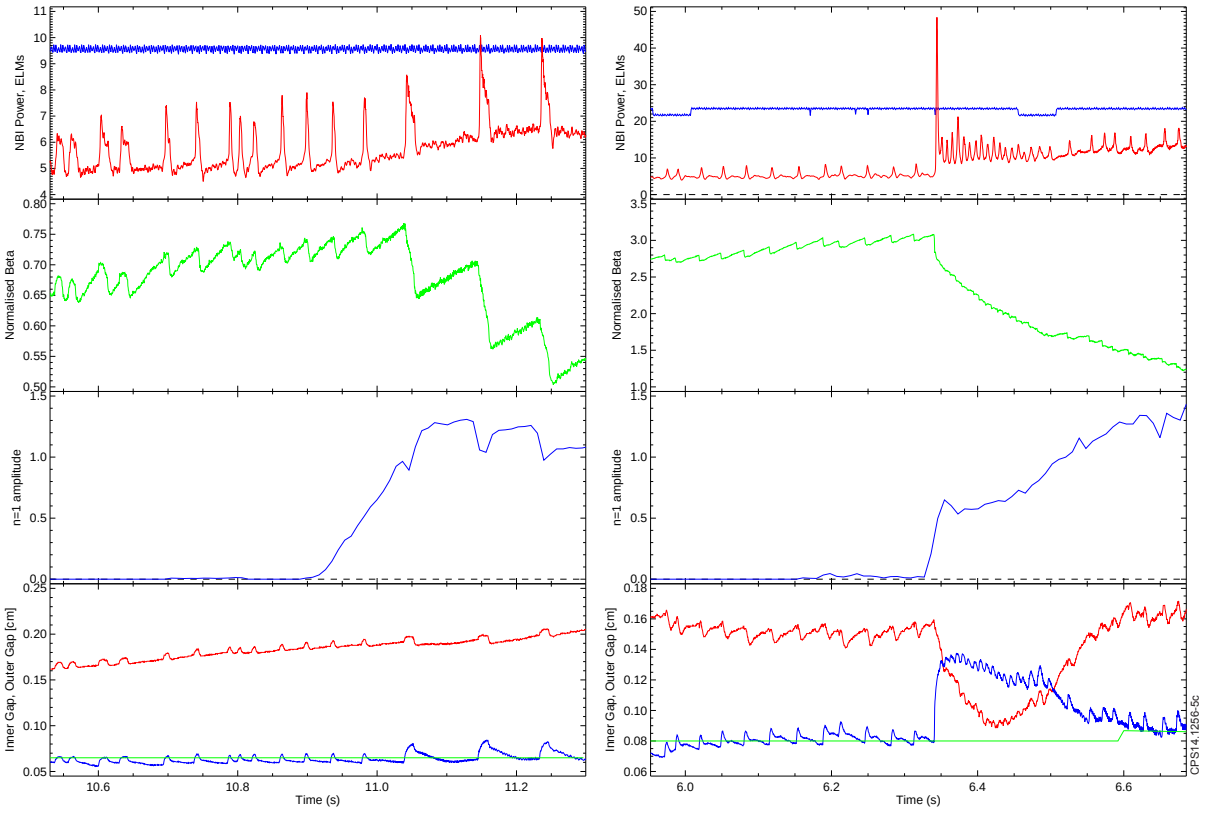

Figure 5. (top pane) The NBI power and the total radiated power measured by the bolometer (showing the ELMs); (second pane) the normalised pressure, β_N; (third pane) the mode ampitude found from magnetics; and (fourth pane), the inner gap (red) and outer gap (blue) from EFIT reconstruction using fast magnetics, compared to the requested outer plasma position (green) used in the plasma control system. On the left is JET shot 84692 which has a long-lasting $n = 1$ kink mode, and on the right is shot 83521 which has an $n = 1$ kink mode triggered by a large ELM event.

should be noted that in the spherical tokamak, the $q = 1$ surface is very broad and near to the plasma edge. To investigate the edge displacement in a conventional aspect-ratio machine, the corrugation due to core MHD in hybrid plasmas in JET [2, 3] has been investigated. Across a database of JET hybrid plasmas, the spontaneously-occurring continuous $n = m = 1$ ideal kink mode, which often occurs with the characteristic low-shear q-profile, never causes a discernible edge displacement. This is exemplified by figure 5, where a typical JET hybrid discharge, shot 84692, is shown to have a long-lasting $n = 1$ kink mode, but no change in the outer gap between the plasma edge and the wall measured by the fast magnetic signals. The only occasion when non-transient boundary displacements are observed is when a large ELM event (see reference [25]) triggers an $n = 1$ mode, with the plasma control system taking approximately an energy confinement time to recover the desired boundary position. An example of this is shown in figure 5.

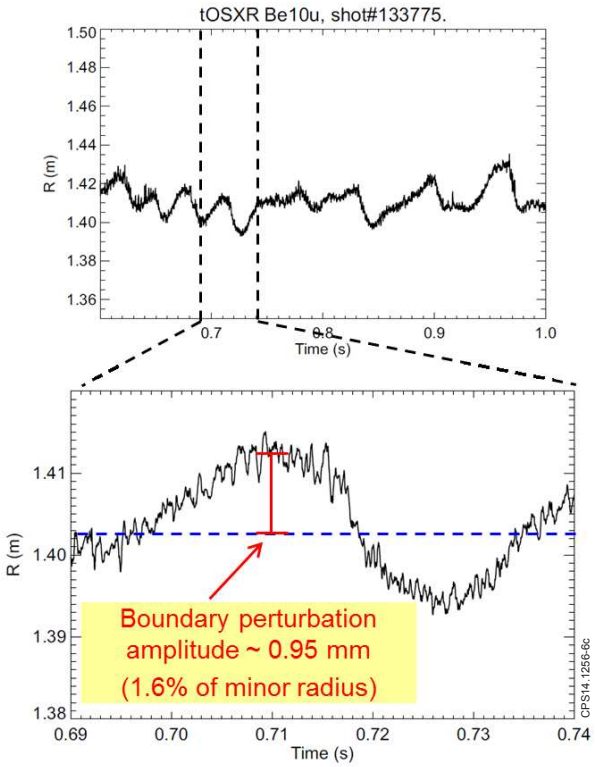

Figure 6. The plasma boundary measured by the Multi-Energy Soft X-ray system in NSTX for a discharge with an n=1 external kink/RWM, showing a displacement of 1.6% of the minor radius.

2.2. NTMs and external $n = 1$ kink modes

Large displacements are also measured in the case of less core-localised MHD instabilities. High normalised pressure plasmas often exhibit saturated global $n = 1$ kink instabilities, or resistive wall modes, which can persist for long times in the presence of magnetic feedback [13]. Whilst this low frequency mode activity is global and perturbs the plasma core, it also gives rise to significant shifts of the plasma boundary. Figure 6 shows the plasma boundary in NSTX, again diagnosed by the SXR camera, showing a displacement of ± 0.95cm, or $\pm 1.6\%$ of the minor radius, when there is a saturated $n = 1$ kink mode in a high β_N plasma.

Naively one might expect the distortion to scale with the normalised pressure as the fluid drive for the instability is increased. However, there is no correlation between the boundary displacement in the presence of such global $n = 1$ instabilities and the normalised pressure with respect to the no-wall limit. Figure 7 shows that the edge displacement is largely independent of β_N. Actually, this is not unexpected since it has been shown that RWM stability depends sensitively on rotation and l_i as well as normalised pressure, and often plasmas at intermediate levels of rotation (ie neither the fastest nor slowest rotating cases in NSTX, nor the plasmas with highest NBI-driven β_N) have the least stable modes as the kinetic damping is minimised [13, 26].

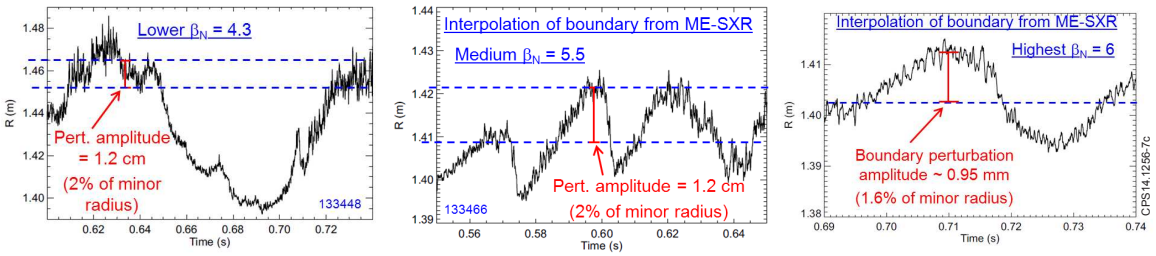

Figure 7. The plasma boundary measured by the Multi-Energy Soft X-ray system in NSTX for a discharge with an n=1 external kink/RWM at (left) β_N less than the no-wall limit, (middle) intermediate normalised pressure and (right) for high β_N above the no-wall limit

Conversely MAST plasmas below the no-wall limit exhibit a strong dependence of the edge displacement on the plasma rotation. Linear CCD cameras have been used to measure D_α light generated by plasma electron impact excitation of the neutral gas outside the separatrix. These midplane cameras are oriented so that the pixel array can see the plasma boundary on both the high- and low-field side. There is some uncertainty in the position of the edge of the plasma inferred from the peak of the D_α emission [27] though qualitative differences between the different phases of the rotating mode are reliable. The Thomson Scattering system on MAST [28] has a radial resolution < 10mm allowing detailed diagnosis of the electron density and temperature profiles. It was designed to achieve low systematic and random errors, allowing observation of changes in the gradients over narrow regions such as the edge pedestal. The displacement as measured by the D_α camera or the Thomson scattering clearly increases as the plasma rotation falls. Figure 8 shows the edge displacement due to NTMs as a function of the core plasma rotation velocity, illustrating largest boundary shifts for the slowest rotating plasmas.

3. Modelling of displacements due to core MHD in present machines

Saturated core instabilities such as those shown in section 2.1 can be modelled using three dimensional equilibrium codes, where the naturally-occurring helical core solution of a 3D equilibrium code is essentially the same as that from a non-linear MHD code (departing from an initially axisymmetric equilibrium) [7]. The ANIMEC code [29] (an anisotropic version of the ideal 3d equilibrium code, VMEC [30]) has been used to simulate the boundary displacements expected in MAST when a helically displaced core is found in the equilibrium solution. Providing a reversed shear q-profile is used, and providing q_{min} is sufficiently close to unity, two equilibria are found: One axisymmetric equilibrium, and the other a helical equilibrium with dominant $m = n = 1$ structure [31, 24, 32, 7]. The three dimensional, helical equilibrium can have slightly lower energy than its axisymmetric neighbour, and so it is in this sense, a preferred state. One can consider the saturated state of a non-linear MHD code equivalent to a 3D equilibrium

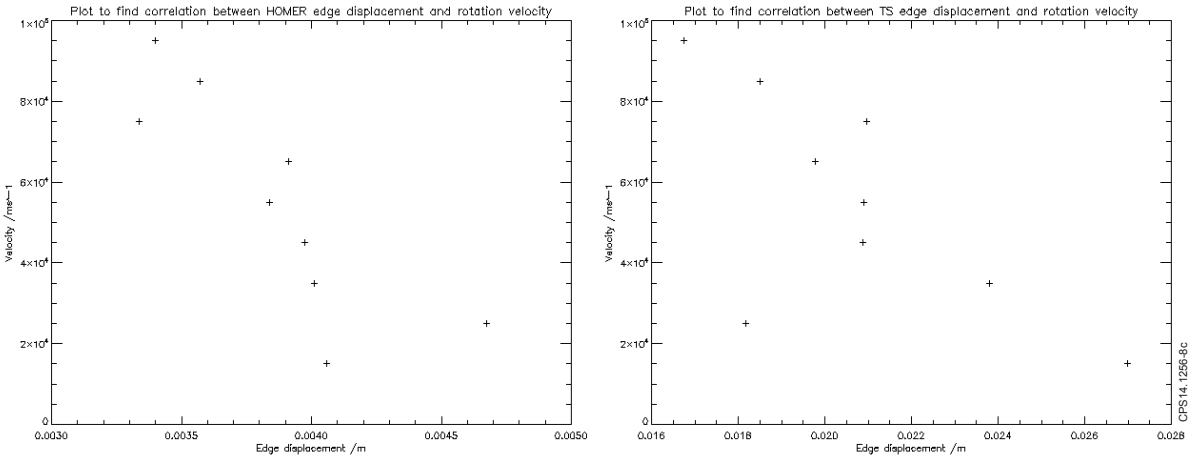

Figure 8. The edge displacement due to NTMs in MAST as measured by (left) the linear D_α camera and (right) Thomson scattering, as a function of the toroidal velocity of the plasma, showing that the boundary shifts increase as the rotation decreases.

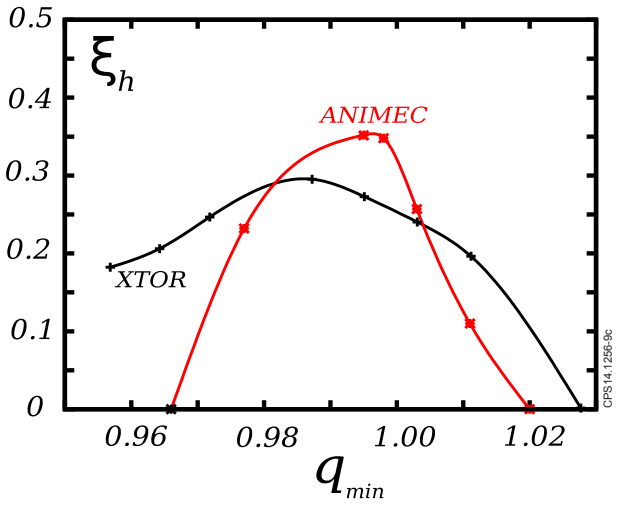

Figure 9. The displacement of the axis in ITER hybrid scenario as a fraction of the minor radius as a function of the minimum safety factor as predicted by nonlinear MHD code, XTOR, showing good agreement with 3d equilibria produced by ANIMEC.

[7]. This is exemplified by figure 9 which, for $q_{min} \geq 1$, shows good agreement of the amplitude of the core displacement due to an $n = 1$ kink mode in a low-shear $q \geq 1$ 'hybrid' scenario as found by a nonlinear MHD code, XTOR [8], compared to that found in a 3d equilibrium analysis using ANIMEC.

The midplane boundary position predicted by ANIMEC is shown as a function of toroidal angle for a MAST plasma which exhibits a long-lived core kink mode [1] in figure 10. It is evident that the edge displacement caused by the core non-axisymmetry is negligible, and indeed smaller than the corrugation due to toroidal field ripple, which itself is much smaller than the perturbation due to applied resonant magnetic

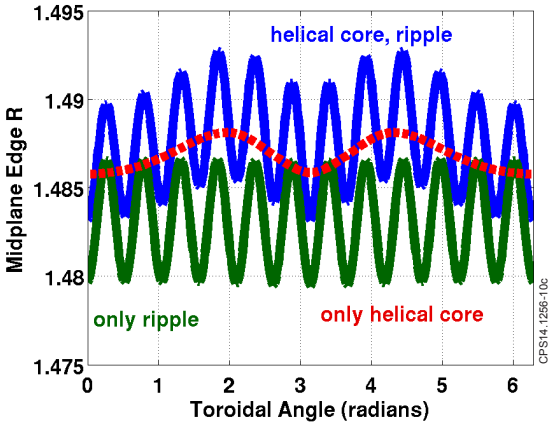

Figure 10. The midplane boundary position as a function of toroidal angle as modelled with ANIMEC for a MAST plasma with toroidal field ripple (green), a helical core (red), or both ripple and a helical core (blue).

perturbations used for controlling edge localised modes [33].

Figure 11 exemplifies the relative insensitivity of the boundary displacement to the amplitude of the helical core, as parameterised by the value of q_{min} which dictates the susceptibility of the equilibrium to a non-axisymmetric branch. The boundary corrugation is of similar amplitude despite the helical core amplitude varying. The equilibrium is most susceptible to an internal kink for q_{min} just above unity [34], and for $q_0 = 0.96, 1.05$ the saturated kink mode amplitude is smaller, yet the boundary displacement is relatively unchanged. The amplitude of the boundary displacement predicted by 3d equilibrium reconstruction exhibiting a helically displaced plasma core is in good agreement with that measured in the presence of a saturated kink mode. Furthermore, the boundary displacement is largely independent of the plasma pressure or the exact value of q_{min} (provided of course that q_{min} is in the range for which a helical core equilibrium is found), as also seen in the experimental data. However, there is a strong dependence of the edge displacement on the edge current [34], which is not borne out experimentally, as the boundary shift is insensitive to the pedestal temperature, and hence bootstrap current.

Similar saturated core instabilities can be analysed using nonlinear MHD codes. Such nonlinear MHD simulation has been performed using the M3D-C^1 code [35] for an NSTX plasma which exhibits a saturated core kink instability [36] (such as that which gives rise to the boundary displacement shown in figure 1). Figure 12 shows the electron temperature profiles before the onset of the kink mode compared to a time when the mode has a saturated amplitude. It is clear that whilst the core of the plasma is cooled and deformeded by the saturated kink mode, the boundary is negligibly affected. This is in good agreement with the measured displacement in NSTX (figure 1) which is less than 1cm.

It should be noted that the simulations presented here are for non-rotating plasmas,

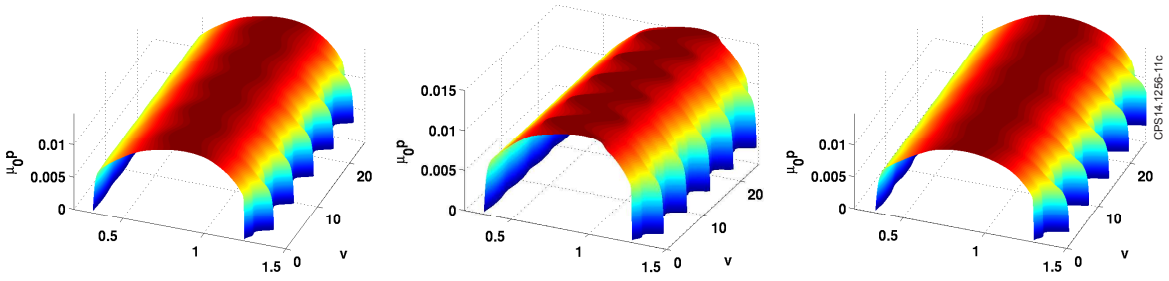

Figure 11. The plasma pressure as a function of radius and toroidal angle as modelled by ANIMEC for MAST plasmas with (left) $q_0 = 1.05$, (centre) $q_0 = 1.00$ and (right) $q_0 = 0.96$. In all cases there is a helical core, although its amplitude is maximised for $q_0 = 1.0$ and a corresponding boundary displacement.

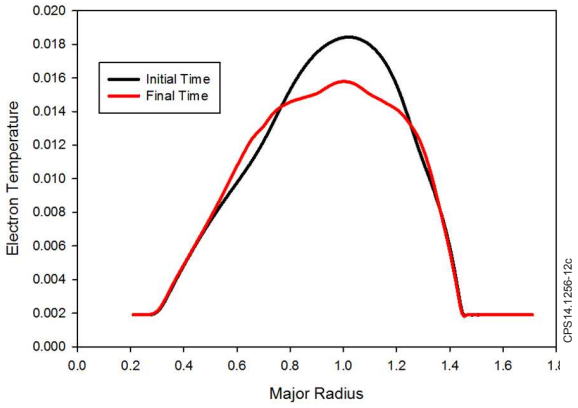

Figure 12. The electron temperature profiles in M3D-C^1 simulations of an NSTX plasma exhibiting a core kink instability, showing a large core displacement, but negligible change in the boundary position.

whereas figure 4 shows that the displacement caused by a saturated $n/m = 1/1$ kink in MAST strongly depends on the plasma rotation velocity. Simulations of 3d equilibria with toroidal flows included will be the subject of future work.

4. Modelling of displacements due to core MHD in ITER

As discussed in section 2, the plasma scenario which is most prone to long-lasting saturated MHD is the so-called 'hybrid' or advanced inductive scenario due to the broad, low shear region in the q-profile and higher normalised pressure. Of course, the baseline scenario is expected to experience MHD instabilities in the core, notably sawtooth oscillations, which could give rise to neoclassical tearing modes, both of which can lead to displacements of the plasma boundary. However, in the case of sawteeth the displacements are small and transient, and for NTMs the confinement degradation is a much more serious issue than whether the boundary is deformed. In comparison, the

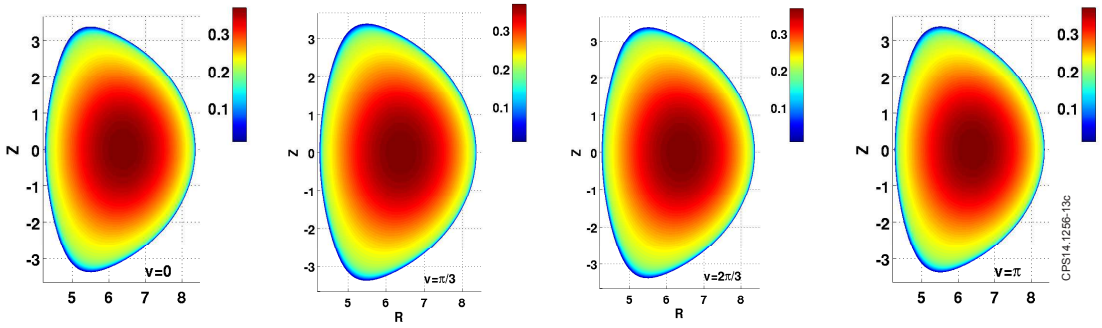

Figure 13. The pressure for the ITER hybrid scenario as predicted by ANIMEC for the axisymmetric equilibrium branch at $\phi = 0, \pi/3, 2\pi/3, \pi$.

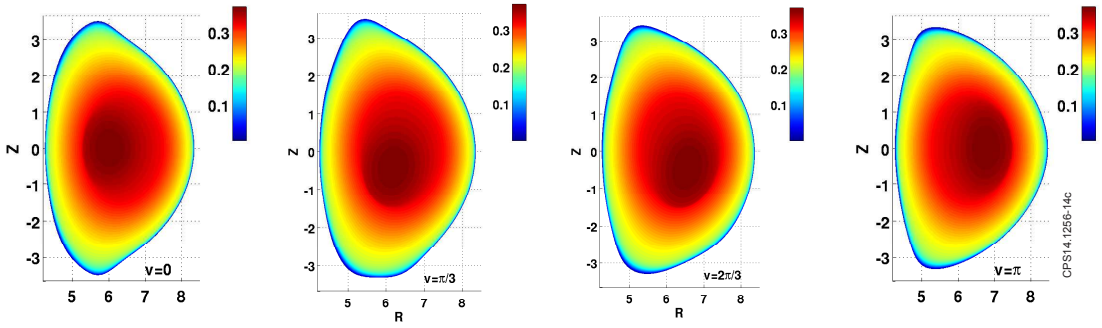

Figure 14. The pressure for the ITER hybrid scenario as predicted by ANIMEC for the helical core branch at $\phi = 0, \pi/3, 2\pi/3, \pi$.

saturated core MHD experienced in hybrid plasmas is usually not overtly detrimental to the plasma performance in large aspect ratio tokamaks, but can last for many energy confinement times, and can lead to enduring displacements of the boundary which could result in difficulties for the plasma control system or for cycling of heat loads on plasma facing components. Therefore, it is the boundary corrugation experienced in the ITER hybrid scenario which we analyse numerically in this section.

The current density profile used in ANIMEC has been tailored in order to give a slightly reversed shear safety factor profile, though actually, the reverse shear is not a strong constraint on the results presented here and qualitatively similar results would be obtained for a flat, low-shear profile provided $q_{min} \approx 1$. Figure 13 shows the plasma pressure for the hybrid scenario equilibrium generated by ANIMEC for the axisymmetric branch, whilst figure 14 shows the pressure for a helical core branch of the equilibrium. It is clear that although the edge flux surfaces are barely perturbed, the plasma core can be significantly distorted when there is an $n = m = 1$ kink in the plasma core. Such a helical core would be expected to manifest itself as the long-lasting ideal perturbations observed in such 'hybrid' scenarios in MAST [1], JET [2], NSTX [4], TCV [6, 7] and EAST [5].

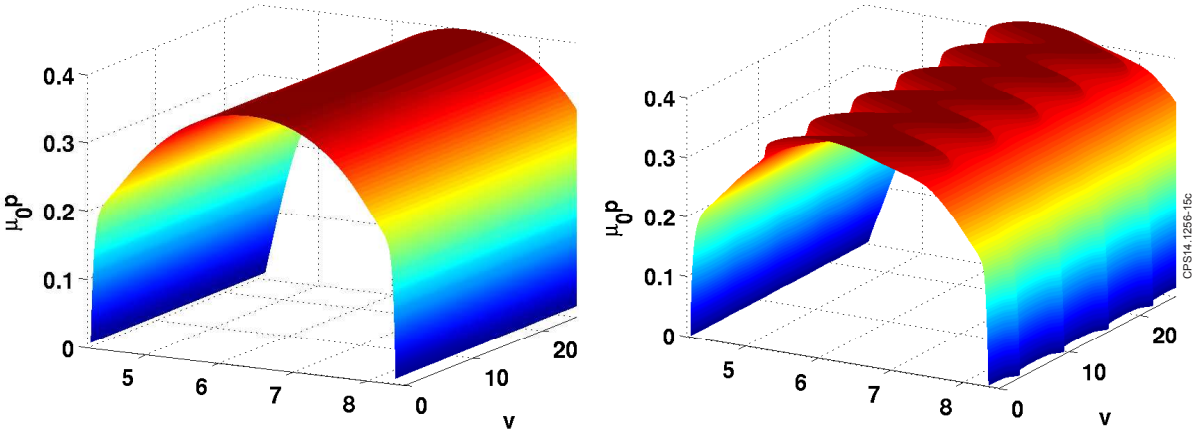

Figure 15. The plasma pressure as a function of radius and time for (left) the axisymmetric case and (right) the helically displaced core for the ITER hybrid scenario, showing the $n = 1$ helical core and the perturbation to the edge position.

This boundary displacement in the presence of an $n = m = 1$ helical core is illustrated clearly in figure 15 where it can be seen that the two neighbouring states of equilibria found with ANIMEC lead to very different toroidal dependence of the plasma boundary. In the axisymmetric equilibrium, there is no corrugation of the boundary, whereas the helical core state, which is equally energetically favourable, gives rise to a $\pm$3cm $n = 1$ distortion of the boundary.

A comparable analysis has been performed using the nonlinear MHD code, M3D-C^1. It is worth recalling that the saturated state of an MHD instability found from an axisymmetric equilibrium is tantamount to a 3d equilibrium state for these hybrid profiles, as shown in figure 9 and reference [7] for the case of a fixed boundary. The electron temperature perturbation predicted by M3D-C^1 at different toroidal positions for the ITER hybrid scenario with realistic bootstrap current is shown in figure 16. Whilst there is a large $n = 1$ perturbation in the plasma core, there is negligible change in the position of the plasma boundary. Differences from ANIMEC could be explained in part by different treatment of the free boundary.

The fact that these two models, be it either a 3d equilibrium reconstruction using ANIMEC or a nonlinear MHD simulation with M3D-C^1, have given good agreement with measured edge displacements due to saturated core MHD instabilities in MAST and NSTX respectively, means that the expected displacement in ITER is likely to lie within the bounds of the predictions from these simulations. That is to say, the displacement in ITER hybrid scenarios due to saturated kink modes prevalent with low-shear and $q_{min} \approx 1$ is in the range $\xi_{MHD} \in \pm[0, 3]$cm, equating to $\xi_{MHD} \in \pm[0, 0.015a]$. Whilst this is not insignificant, it is within the acceptable bounds of the boundary displacement allowable in ITER for both plasma control to be effective and heat loads to the plasma facing components to be manageable.

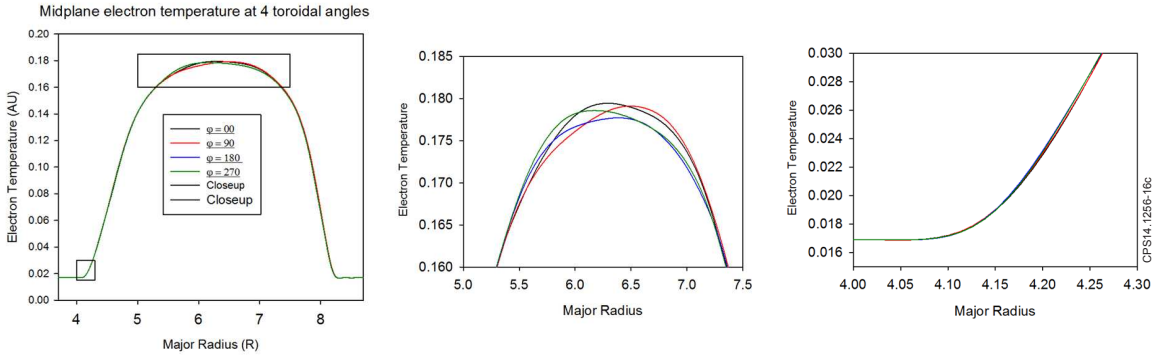

Figure 16. The electron temperature profile at four different toroidal positions for an ITER hybrid plasma as predicted by the M3D-C^1 code for (left) the whole major radius, (centre) the core plasma showing an $n = 1$ kink mode and (right) the pedestal, showing negligible boundary displacement.

5. Discussion and Conclusions

It is evident that saturated MHD instabilities can give rise to significant displacements of the plasma boundary. These displacements have been measured in various tokamaks and successfully compared with numerical simulation, notwithstanding the approximation of static plasmas, whilst the rotation is seen empirically to affect the edge plasma displacement caused by saturated kink modes. Good agreement has been found between these experimental measurements and numerical simulation – either ideal three dimensional MHD equilibrium reconstruction or nonlinear MHD modelling – giving credence to the application of such simulations for extrapolation to ITER. The boundary displacement resultant from core MHD instabilities in ITER is predicted to be less than $\pm 1.5\%$ of the minor radius.

Such toroidal corrugation of the plasma boundary affects many things, notably the coupling of ICRH, the minimum values of wall gaps assumed for safe operation, the plasma position control, and the control of ELMs. Whilst a displacement of ± 3cm in the baseline scenario is allowable from both a plasma control and heat loading perspective, it is important to realise that such displacements may occur and plan for the plasma control system and heating actuators to be able to account for such distortions safely.

Acknowledgements

This work was conducted under the auspices of the ITPA MHD Stability Topical Group. This work was partly funded by the RCUK Energy Programme [grant number EP/I501045]; the European Communities under the contract of Association between EURATOM and CCFE, CRPP and ENEA; and US Department of Energy under DE-AC02-09CH11466. To obtain further information on the data and models underlying this paper please contact PublicationsManager@ccfe.ac.uk. The views and opinions

expressed herein do not necessarily reflect those of the European Commission. This work was carried out within the framework of the European Fusion Development Agreement.

[1] Chapman IT *et al* 2010 *Nuclear Fusion* **50** 045007
[2] Buratti P *et al* 2010 *Nuclear Fusion* **52** 023006
[3] Kwon OJ *et al* 2012 *Plasma Physics and Controlled Fusion* **54** 045010
[4] Menard JE et al, 2006 *Phys. Rev. Lett.* **97** 095002
[5] W. Chen, et. al., *Nucl.Fusion* **50** (2010) 084008
[6] H Reimerdes et al *Plasma Phys Control Fusion* **42** 629 (2006)
[7] Graves JP et al. 2013 *Plasma Phys. Control. Fusion* **55** 014005
[8] H. Lütjens, J.-F. Luciani, D. Leblond, F. Halpern and P. Maget, *Plasma Physics and Controlled Fusion* **51** 124038 (2009)
[9] Baruzzo M et al, 2010 *Plasma Phys. Control. Fusion* **52** 075001
[10] La Haye RJ et al. 2002 *Phys plasmas* **9** 2051
[11] Maraschek, M., et al 2003 *Plasma physics and controlled fusion* **45** 1369
[12] Garofalo, AM et al. 2007 *Nuclear Fusion* **49** 1121
[13] Sabbagh, SA, et al. 2010 *Nuclear Fusion* **50** 025020
[14] Katsuro-Hopkins, O et al. 2007 *Nuclear Fusion* **47** 1157
[15] Bolzonella, T et al. 2008 *Physical Review Letters* **101** 165003
[16] Kocan M, 2013 "Heat loads to the ITER first-wall panels in the ICRH-optimized plasma equilibrium" Tech. rep. ITER DML5YK
[17] JB Lister, A Portone and Y Gribov 2006 *Control Systems* **26** 79
[18] Menard JE et al, 2005 *Nucl. Fusion* **45** 539
[19] Hua MD et al, *European Physics Letters*, **90**, 55001 (2010)
[20] Hua MD et al, *Plasma Physics and Controlled Fusion*, **52**, 035009 (2010)
[21] K.C. Shaing Phys. Plasmas **10**, 1443 (2003)
[22] Avinash, R.J. Hastie, J.B. Taylor and S.C. Cowley, Phys. Rev. Lett. **59**, 2647 (1987)
[23] M.N. Rosenbluth *et al.*, Phys. Fluids **16**, 1894 (1973)
[24] WA Cooper et al, *Plasma. Phys. Control. Fusion* **53** (2011) 024002
[25] YF Baranov et al, *Nucl. Fusion* **52** 023018 (2012)
[26] J.W. Berkery, et al., *Phys Rev Lett* **104** (2010) 035003
[27] MR Tournianski *et al* 2003 *Rev. Sci. Instrum.* **74** 2089
[28] R Scannell *et al* 2008 *Rev. Sci. Instrum.* **79** 10E730
[29] Cooper WA *et al* 2009 *Comput. Phys. Commun.* **180** 1524
[30] Hirshman SP and Lee DK 1986 *Comput. Phys. Commun.* **43** 143
[31] Cooper WA et al, 2011 *Plasma Phys. Control. Fusion* **53** 074008
[32] WA Cooper et al, *Plasma Phys. Control. Fusion* **53** (2011) 124005
[33] IT Chapman et al, 2012 *Plasma Phys Control Fusion* **54** 105013
[34] Cooper WA et al, 2013 *40th EPS Conference on Plasma Physics, Helsinki, Finland*
[35] S. C. Jardin, J. Breslau, N. Ferraro, *J. Comput. Phys* **226** (2007) 2146
[36] Breslau JA et al, 2011 *Nucl. Fusion* **51** 063027